

# Demonstration of Two Independently Folding Domains in the $\alpha$ Subunit of Bacterial Luciferase by Preferential Ligand Binding-Induced Stabilization<sup>†</sup>

Brian W. Noland<sup>‡</sup> and Thomas O. Baldwin\*

Department of Biochemistry & Molecular Biophysics and The Institute for Biomedical Science and Biotechnology,  
The University of Arizona, Tucson, Arizona 85721-0088

Received August 26, 2002; Revised Manuscript Received December 16, 2002

**ABSTRACT:** The  $\alpha$  subunit of bacterial luciferase unfolds and refolds reversibly by a three-state mechanism in urea-containing buffer. It has been proposed that the three-state unfolding of the  $\alpha$  subunit arises from a stepwise unfolding of a C-terminal folding domain at lower concentrations of urea, followed by unfolding of the N-terminal domain at higher concentrations of urea (Noland, B. W., Dangott, L. J., and Baldwin, T. O. (1999) *Biochemistry* 38, 16136–16145). The location of an anion binding site in the proposed N-terminal folding domain allowed the folding mechanism to be probed in the context of the intact polypeptide. Anions preferentially stabilized the N-terminal domain in a concentration-dependent manner. The polyvalent anions sulfate and phosphate were found to be more stabilizing than monovalent chloride ion. Cations did not show a similar stabilizing effect, demonstrating that the stabilization was due to the anions alone. The purified N-terminal domain prepared by limited proteolysis and anion exchange chromatography was found to refold cooperatively with a midpoint approximately that of the second unfolding transition of the  $\alpha$  subunit. Phosphate ion stabilized this fragment to roughly the same extent as it did the  $\alpha$  subunit. The results presented are consistent with the proposed two-domain folding model and demonstrate that anion binding to the N-terminal folding domain stabilizes the  $\alpha$  subunit of bacterial luciferase.

The study of protein folding, stability, and structure has intrigued protein biochemists for over a half-century and today comprises a major component of research in the field. Despite many advances in our understanding of the thermodynamic and kinetic processes involved in protein folding in recent years, a general solution to the protein folding problem remains elusive. Many of the small single-domain proteins often studied as folding models unfold and refold by apparent two-state mechanisms demonstrating a lack of detectable intermediate states. The folding of large, multi-domain or multisubunit proteins is in general more complicated than folding of small single-domain proteins. A solution to the protein folding problem will require an understanding of folding and assembly of large, complicated proteins, as small 2-state folding proteins comprise a minor subset of all proteins.

Wetlaufer has proposed that the folding of larger proteins can be simplified by considering them as collections of smaller folding domains (1). The folding mechanisms of several multidomain proteins have been explored by preparing fragments believed to act as folding domains and

characterizing the folding behavior of the fragments in isolation (see ref 1 for a review).

Bacterial luciferase is an  $\alpha\beta$  heterodimeric enzyme that catalyzes the light-producing reaction in bioluminescent marine bacteria. The subunits are homologous and both adopt the  $(\beta/\alpha)_8$  or TIM barrel fold (2, 3). The refolding behavior of luciferase and its subunits has been investigated by monitoring activity recovery following dilution out of urea containing buffers and also by direct spectroscopic measurements (4–6). From these studies it was learned that the folding of bacterial luciferase is a multistep process involving isomerizations as well as second-order processes. In equilibrium studies, bacterial luciferase was shown to unfold and refold reversibly by a three-state mechanism maximally populating a folding intermediate at ca. 2.1 M urea (7). Protein concentration dependence of the second unfolding transition demonstrates that the equilibrium folding intermediate is dimeric. The loss of enzyme activity as a function of the urea concentration follows the first unfolding transition, demonstrating that the dimeric intermediate is inactive (7).

In the absence of the  $\alpha$  subunit, the  $\beta$  subunit can slowly form a  $\beta_2$  homodimer of exceptional kinetic stability (8). The  $\beta_2$  homodimer is resistant to denaturation in 5 M urea. If the homodimer is first treated with 5 M guanidine and then dialyzed into 5 M urea, the protein remains unfolded (8, 9). Two high-resolution X-ray crystal structures of the  $\beta_2$  homodimer have been reported (10, 11). The  $\beta_2$  structure is remarkably similar to the structure of the bacterial luciferase heterodimer (2, 3), the most notable difference

<sup>†</sup> This work is from the dissertation of B.W.N. submitted to the Graduate College of Texas A&M University, College Station, TX, in partial fulfillment of the requirements of the Ph.D. degree. The work was supported by Grant No. MCB 0078363 from the National Science Foundation to T.O.B.

\* To whom correspondence should be addressed at the Department of Biochemistry & Molecular Biophysics. Phone: (520) 621-9185. Fax: (520) 626-9204. E-mail: tbaldwin@u.arizona.edu.

<sup>‡</sup> Current address: Structural Genomix, 10505 Roselle St., San Diego, CA 92121. E-mail: BNoland@Stromix.Com.

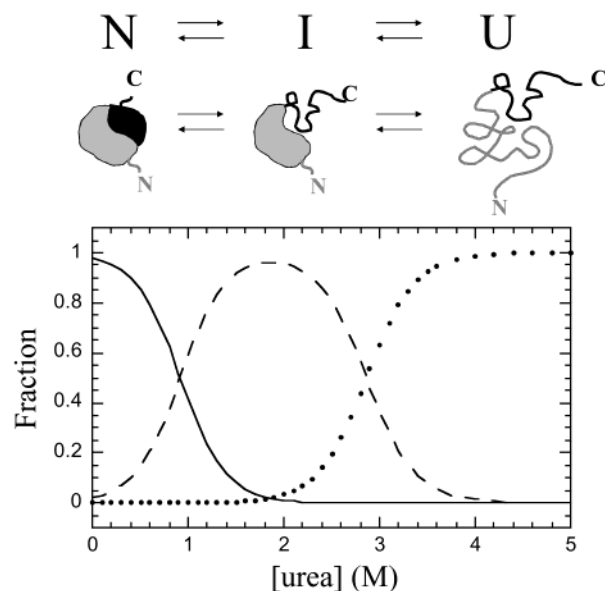


FIGURE 1: Proposed unfolding mechanism for the  $\alpha$  subunit of bacterial luciferase. The unfolding scheme shown is based on a previously proposed model (12). In this model the native to intermediate transition is characterized by the unfolding of a C-terminal domain of the  $\alpha$  subunit. The second step is the unfolding of an N-terminal domain. The plot shown at the bottom is the calculated fraction of each species at equilibrium using a three-state unfolding mechanism and the previously determined free energy parameters (12).

being a somewhat reduced solvent accessible channel at the subunit interface (10, 11). The structure of the kinetically stable  $\beta_2$  species thus offers little to explain the unusual kinetic folding behavior.

Equilibrium denaturation experiments have revealed that the free  $\alpha$  subunit unfolds and refolds by a three-state mechanism, maximally populating a folding intermediate in ca. 2 M urea (Figure 1) (12). Far-UV circular dichroism analysis of the  $\alpha$  subunit intermediate in 2 M urea has shown that the protein loses approximately 40% of the native secondary structure in the intermediate state. The  $\alpha$  subunit in 2 M urea has decreased intrinsic fluorescence with respect to that in buffer without a corresponding red-shift of the emission maximum, revealing that in the intermediate state the tryptophan residues remain largely shielded from solvent. Near-UV circular dichroism studies of the intermediate show that the environment of the aromatic residues changes with respect to the native state but that the core of the protein retains asymmetry. The results of limited proteolysis of the  $\alpha$  subunit in 2 M urea combined with the spectroscopic analysis led to the proposal that the  $\alpha$  subunit unfolds by a stepwise unfolding of a C-terminal domain at low concentrations of urea, followed by the N-terminal domain at higher concentrations of urea (Figure 1) (12). The folding behavior of fragments that approximate the proposed N- and C-terminal folding domains of the  $\alpha$  subunit of bacterial luciferase is consistent with such a model (13).

To test our proposed folding/unfolding mechanism for the  $\alpha$  subunit, we have studied the effects of ligand binding on the urea-induced unfolding transitions. Figure 2 outlines the predicted effects of ligand binding on the proposed N- and C-terminal folding domains of the  $\alpha$  subunit. Assume there is a ligand that specifically binds the C-terminal folding domain of the  $\alpha$  subunit (cartoon beside Figure 2A). On the

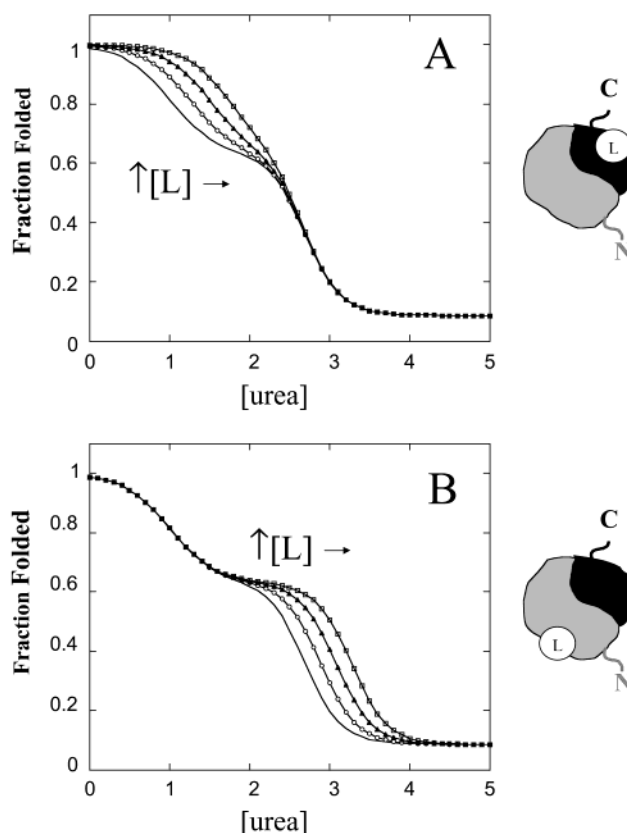


FIGURE 2: Predicted effects of ligand binding linked to the folding of the  $\alpha$  subunit of bacterial luciferase. Panel A shows the predicted effect of increasing ligand concentration on the folding of the  $\alpha$  subunit if the ligand binds the C-terminal domain. The cartoon to the right of the graph shows the ligand binding the C-terminal domain. Panel B shows the predicted effect of increasing ligand concentration on the folding of the  $\alpha$  subunit if the ligand binds the N-terminal domain. The cartoon to the right of the graph shows the ligand bound to the N-terminal domain.

basis of the two-domain folding model, the effect of increasing the ligand concentration would be to stabilize the C-terminal domain and thus cause the midpoint of the first transition to shift to higher urea concentrations (Figure 2A). In this scenario, the second transition would not be affected. Alternatively, consider the case in which the ligand specifically binds the N-terminal folding domain. In this case, the midpoint of the second transition would shift to higher urea concentrations with increasing ligand concentration (Figure 2B) and the first transition would not be affected.

The location of an anion binding site on bacterial luciferase was apparent from the structure determined by X-ray diffraction from crystals grown in the presence of phosphate buffered ammonium sulfate (2). The existence of the anion binding site had previously been suggested on the basis of solution studies (14–16). The multivalent anion appears to interact with Arg107 (2), which also may be the binding site for the phosphate group of the flavin substrate. This binding site appears to be entirely within the proposed N-terminal domain of the  $\alpha$  subunit (Figure 3). On the basis of the prediction outlined in Figure 2B, the effect of increasing the concentration of phosphate or sulfate would be to shift the midpoint of the second folding transition to higher urea concentrations. According to the prediction, the first transition should be unaffected by the increased salt concentration (Figure 2B).

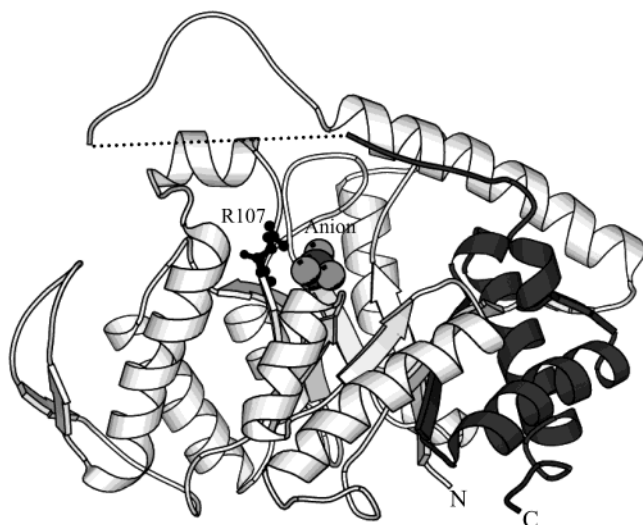


FIGURE 3:  $\alpha$  subunit of bacterial luciferase with bound anion. The  $\alpha$  subunit is rendered in ribbon diagram from the 2.4 Å luciferase heterodimer crystal structure (2). The proposed N- and C-terminal domains are colored light and dark gray, respectively. The N- and C-terminal portions of the protease labile loop are connected by a straight dotted line to indicate the disordered portion of the structure from Phe272 to Thr288. The anion is annotated and shown bound to the proposed N-terminal domain. The guanido group of arginine 107 is shown in black ball-and-stick model and is assumed to be the only side chain ligand bound to the anion (2). The image was created using SPOCK (53) and MOLESCRIPT (54).

In the studies reported here, the equilibrium unfolding and refolding of the  $\alpha$  subunit was investigated in the presence of various ionic ligands. Multivalent anions dramatically shifted the position of the second transition to higher denaturant concentrations. The results presented are consistent with stabilization arising from specific ion binding rather than nonspecific salt effects. Cations did not show a similar stabilizing effect suggesting that the observed stabilization was due to anion binding alone. The stabilizing effect of the salts appeared to arise from anion binding to the proposed N-terminal folding domain of the  $\alpha$  subunit. These studies further provide further evidence in support of the previously proposed 2-domain folding model for the  $\alpha$  subunit of bacterial luciferase.

## MATERIALS AND METHODS

**Materials.** The  $\alpha$  subunit of bacterial luciferase from *Vibrio harveyi* was expressed and purified from *Escherichia coli* strain ALF1 as previously described (12). Ultrapure urea was purchased from ICN. TLCK<sup>1</sup>-treated chymotrypsin was purchased from Worthington Enzymes. Dithiothreitol (DTT) was purchased from Boehringer Mannheim, and  $\text{NaH}_2\text{PO}_4$  and  $\text{K}_2\text{HPO}_4$  from J. T. Baker. All other chemicals were reagent grade or better.

**Preparation and Purification of Proteolytic Fragments.** The limited proteolysis of bacterial luciferase has been studied in detail; the initial cleavage with chymotrypsin occurs at 2 sites, the peptide bonds following residues 280 and 282 (17, 18), producing an N-terminal fragment of the

$\alpha$  subunit (the  $\sim 28$  kDa  $\gamma$  fragment) and the C-terminal  $\delta$  fragment. The  $\gamma$  fragment was used in these studies as the model for the N-terminal domain of the  $\alpha$  subunit. Bacterial luciferase from *V. harveyi* was expressed from *E. coli* strain IGC1 and purified as previously described (19, 20). Prior to digestion, 300 mg of luciferase was incubated at 18 °C in 30 mL of 50 mM phosphate buffer, pH 7.00, 1 mM DTT. Chymotrypsin was added from a 10 mg/mL stock so that the molar ratio of luciferase to chymotrypsin was 100:1. The progress of the digestion was monitored by the loss in bioluminescence activity as a function of time. When 1% of the activity remained, PMSF<sup>2</sup> in 2-propanol was added to give a  $\sim 100$ -fold molar excess over the chymotrypsin concentration to quench the reaction. The digest was then diluted 1:1 with 10 M urea to bring the urea concentration to 5 M. The digest was dialyzed against three changes of 20-fold excess 10 mM phosphate buffer containing 5 M urea at 4 °C. The dialyzed sample was then loaded onto a 75 mL Q-sepharose (Pharmacia) column equilibrated with 10 mM phosphate buffer plus 5 M urea at pH 7.00. The fragments were eluted using a linear gradient from 10 to 200 mM phosphate over 5–10 column volumes and fractionated for analysis and pooling. Fractions containing the  $\gamma$  fragment were pooled on the basis of SDS-PAGE<sup>1</sup> analysis of the Q-sepharose column fractions, concentrated to between 5 and 10 mg/mL and flash frozen under liquid  $\text{N}_2$ .

**Equilibrium Denaturation Experiments.** Equilibrium denaturation experiments were performed as previously described (12) but in 50 mM MOPS,<sup>1</sup> pH 7.00, 1 mM DTT, and the indicated concentration and type of salt. Fluorescence emission was monitored using an SLM-Aminco 8000C spectrofluorometer using a 1 cm quartz cuvette thermostated to 18 °C by a circulating water bath. Emission spectra were analyzed over the wavelength range of 310–430 nm using an excitation wavelength of 295 nm. Spectra were corrected for background signal contribution. Center of mass wavelength (CMW) was measured from fluorescence emission spectra. The CMW was calculated using eq 1 (21), where  $F_i$  is the fluorescence intensity at wavelength  $\lambda_i$ . Unlike fluorescence measured at a single wavelength, CMW is an integral measurement and is less susceptible to intensity-dependent noise (21). Urea denaturation midpoints ( $C_{\text{mid}}$ ) were determined for the  $\alpha$  subunit by fitting equilibrium denaturation to a three-state unfolding model as previously described (12). Urea denaturation midpoints for the  $\gamma$  fragment refolding data were determined by fitting the data to a two-state unfolding model as previously described (22).

$$\text{CMW} = (\sum F_i \lambda_i) / \sum F_i \quad (1)$$

**Analytical Ultracentrifugation.** Sedimentation equilibrium experiments were carried out using Beckman XL-I analytical ultracentrifuge. Samples were dialyzed through three changes at 4 °C against 50 mM MOPS buffer, pH 7.00, 1 mM DTT, and 100 mM or 500 mM  $\text{NaH}_2\text{PO}_4$ ,  $\text{Na}_2\text{SO}_4$ , or NaCl. The dialyzed samples were spun at 15 000 rpm at 18 °C until equilibrium was achieved (approximately 20 h). At equilibrium the absorbance at 280 nm was measured as a function of radial position with a radial step size of 0.001 cm. The resulting data were analyzed using eq 2, which describes

<sup>1</sup> Abbreviations: TLCK, 1-chloro-3-(tosylamido)-7-amino-2-heptanone; PMSF, phenylmethanesulfonyl fluoride; SDS-PAGE, sodium dodecyl sulfate polyacrylamide gel electrophoresis; MOPS, 3-(N-morpholino)propanesulfonic acid; CMW, center of mass wavelength.



the behavior of a monomer–dimer associating system:

$$A_r = A_0 \exp\{[M(1 - \nu\rho)\omega^2/2RT][r^2 - r_0^2]\} + (A_0)^2 K_a \exp\{[2M(1 - \nu\rho)\omega^2/2RT][r^2 - r_0^2]\} + E \quad (2)$$

Here  $A_r$  = the absorbance at any radial position  $r$ ,  $r$  = the radial position,  $A_0$  = the absorbance at the reference radial position  $r_0$ ,  $r_0$  = reference radial position,  $K_a$  = association equilibrium constant,  $\nu$  = partial specific volume of the sedimenting species,  $\rho$  = solvent density,  $\omega$  = angular velocity,  $R$  = the ideal gas constant, and  $T$  = absolute temperature. The partial specific volume,  $\nu$ , for the  $\alpha$  subunit, 0.731 mL/g, was calculated on the basis of the amino acid composition (17) as described by Cohn and Edsall (23). The value of  $\rho$  was calculated from standard tables (24). Sedimentation equilibrium data were analyzed using eq 2 with the nonlinear least-squares fitting engine in the program Kaleidagraph (Synergy Software, Reading, PA). The value of  $M$ , 40 153 Da calculated from the amino acid composition of the protein, was held constant in the fitting process.

**Chymotrypsin Proteolysis.** Limited proteolysis of the  $\alpha$  subunit of bacterial luciferase was performed as described previously (12) but in 50 mM MOPS, pH 7.00, 1 mM DTT, and the indicated salt conditions. SDS–PAGE gels were digitized at a resolution of 200 dpi, and the density associated with each protein band was measured with Scion Image, a modified form of NIHImage for the PC (Scion Corp., Frederick, MD). The pseudo-first-order rate constant for the initial chymotrypsin cleavage event of the  $\alpha$  subunit was obtained from a nonlinear least-squares fit of eq 3 to the density associated with the  $\alpha$  subunit as a function of digest time, where  $D_t$  is the protein density at time  $t$ ,  $D_0$  is the initial density,  $D_\infty$  is the density at infinite time,  $k$  is the first-order rate constant in reciprocal minutes, and  $t$  is the digestion time in minutes. Nonlinear regression was performed with Kaleidagraph (Synergy Software, Reading, PA).

$$D_t = (D_0 - D_\infty)e^{-kt} + D_\infty \quad (3)$$

## RESULTS

**Effect of Different Anions on the Folding Behavior of the  $\alpha$  Subunit.** Figure 4A shows unfolding transitions monitored by fluorescence in the presence of 0 to 400 mM sodium phosphate in 100 mM increments. The first transition was largely unaffected, but there was a considerable effect on the second transition. Panel B of Figure 4 shows the unfolding in buffer and 200 and 400 mM  $\text{Na}_2\text{SO}_4$ . Again, the first transition was salt independent but the second transition was affected even more than with sodium phosphate. Figure 4C shows unfolding curves for the  $\alpha$  subunit in buffer and 200 and 400 mM  $\text{NaCl}$ . The first unfolding transition was unaffected, as in panels A and B, and there was only a slight effect on the second transition. There was a striking difference in the ability of the multivalent anions to stabilize the second transition compared with monovalent chloride ion. Figure 5A shows the effect of salt concentration on the observed midpoint of the second unfolding transition for the various sodium salts tested. Sulfate was most stabilizing, followed by phosphate and chloride. If the same data were plotted against ionic strength rather than salt concentration, the same stabilization distribution was ob-

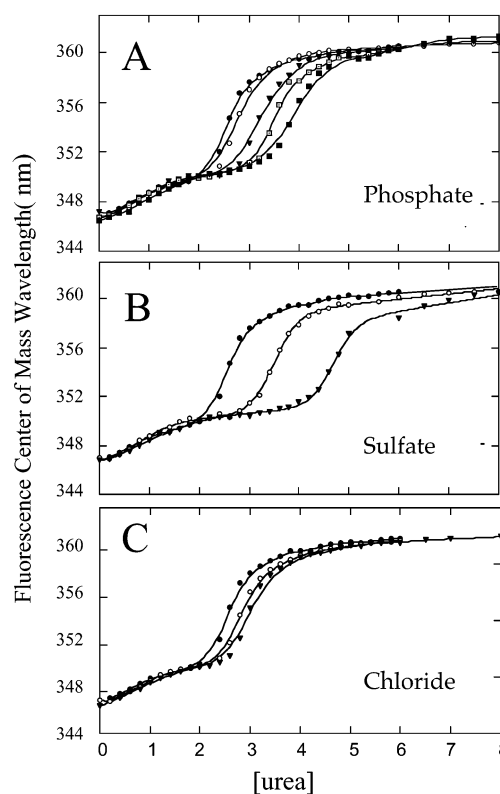


FIGURE 4: Effect of sodium salts on the equilibrium denaturation behavior of the  $\alpha$  subunit. The three panels above show the equilibrium denaturation of the  $\alpha$  subunit with increasing concentrations of various sodium salts monitored by fluorescence CMW with excitation at 295 nm. Panel A shows  $\alpha$  subunit unfolding curves in buffer (●), 100 mM phosphate (○), 200 mM phosphate (▼), 300 mM phosphate (□), and 400 mM phosphate (■). Panel B is the unfolding of the  $\alpha$  subunit in buffer (●), 200 mM sulfate (○), and 400 mM sulfate (▼). Panel C shows  $\alpha$  subunit denaturation curves collected in buffer (●), 200 mM chloride (○), and 400 mM chloride (▼). The curves were fully reversible in every salt concentration shown, but these controls are not shown for the sake of clarity.

tained (Figure 5B). The observed effect on the second unfolding transition was not simply an ionic strength effect but likely arose from specific ion binding.

**Effect of Different Cations on the Folding of the  $\alpha$  Subunit.** The effect of various cations on the folding behavior of the  $\alpha$  subunit was tested under conditions of constant sulfate concentration (Figure 6). Denaturation curves in 200 mM  $(\text{NH}_4)_2\text{SO}_4$ ,  $\text{Na}_2\text{SO}_4$ , or  $\text{K}_2\text{SO}_4$  overlay indicating roughly the same stabilizing effect for ammonium, sodium, and potassium ions. The denaturation curve for 200 mM  $\text{MgSO}_4$  showed no change for the first transition and a more shallow second transition with a midpoint at a slightly lower concentration of urea. The shallowed second transition observed with  $\text{MgSO}_4$  might indicate a change in the unfolding mechanism. These results suggest that the observed salt effect on the second unfolding transition does not depend appreciably upon the cation.

**Effect of Phosphate on the Folding of the N-Terminal Folding Domain.** The  $\gamma$  fragment was prepared by limited chymotryptic proteolysis of the free  $\alpha$  subunit of luciferase and well-approximates the proposed N-terminal folding domain (the light gray portion of the protein in Figure 3). The equilibrium denaturation of the  $\gamma$  fragment in buffer and buffer supplemented with 400 mM sodium phosphate is

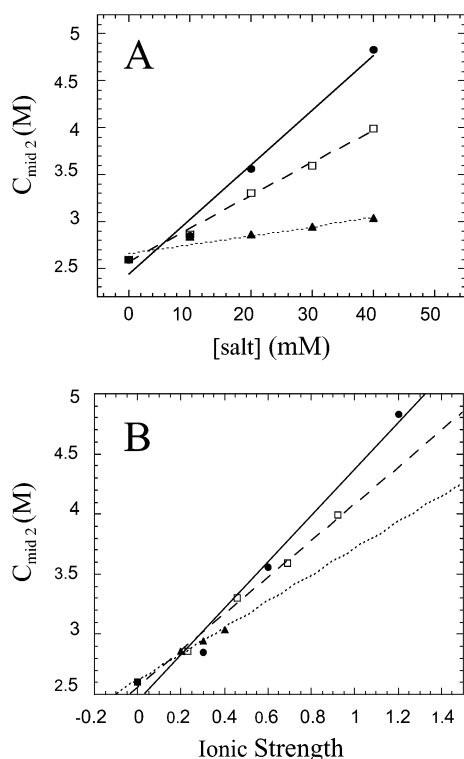


FIGURE 5: Midpoint of the second  $\alpha$  subunit unfolding transition as a function of salt concentration. Panel A shows the midpoint of the second  $\alpha$  subunit unfolding transition as a function of salt concentration for sodium sulfate ( $\bullet$ ), sodium phosphate ( $\square$ ), and sodium chloride ( $\blacktriangle$ ). Panel B shows the same data plotted as a function of the ionic strength.

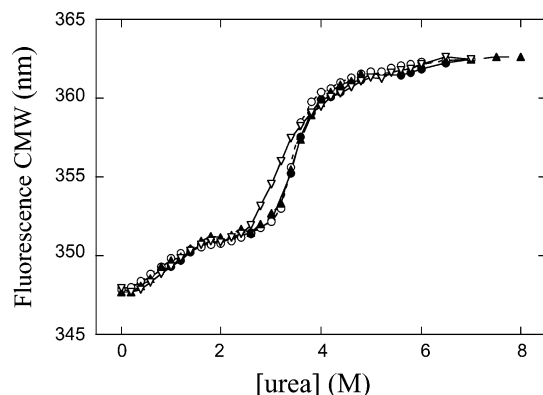


FIGURE 6: Effect of cations on the equilibrium denaturation behavior of the  $\alpha$  subunit. Shown above are equilibrium denaturation curves in 200 mM  $K_2SO_4$  ( $\bullet$ ), 200 mM  $(NH_4)_2SO_4$  ( $\circ$ ), 200 mM  $Na_2SO_4$  ( $\blacktriangle$ ), and 200 mM  $MgSO_4$  ( $\nabla$ ). Denaturation was monitored by fluorescence CMW with excitation at 295 nm. Refolding controls show that the presence of the salts does not affect the reversibility of the process but are not shown for the sake of clarity.

shown in Figure 7A. As would be predicted from the proposed folding mechanism, elimination of the C-terminal folding domain causes apparent two-state unfolding with a midpoint that corresponds to the second unfolding transition midpoint of the  $\alpha$  subunit (Figures 4 and 7). Because the N-terminal domain contains the anion binding site, it would be predicted that the  $\gamma$  fragment would also be stabilized in the presence of increasing concentration of anions. As predicted, the  $\gamma$  fragment was stabilized by the addition of 400 mM sodium phosphate. The observed stabilization of the  $\gamma$  fragment by phosphate was approximately the same

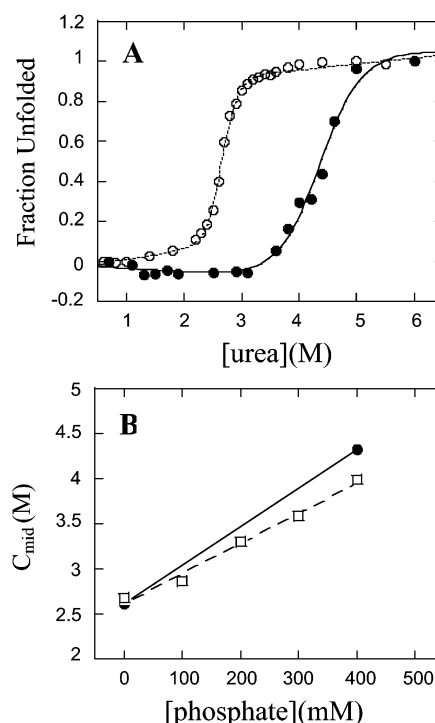


FIGURE 7: Effect of phosphate on the folding of the  $\gamma$  fragment of the  $\alpha$  subunit. Panel A: Equilibrium refolding of the  $\gamma$  fragment at a protein concentration of 20  $\mu$ g/mL from buffer ( $\circ$ ) and from buffer with 400 mM sodium phosphate ( $\bullet$ ). The lines through the data represent fits to a two-state unfolding function for the determination of the midpoint of denaturation. Panel B: The midpoint of the refolding curves for the  $\gamma$  fragment ( $\bullet$ ) and the midpoint of the second  $\alpha$  subunit unfolding transition ( $\square$ ) as a function of phosphate concentration.

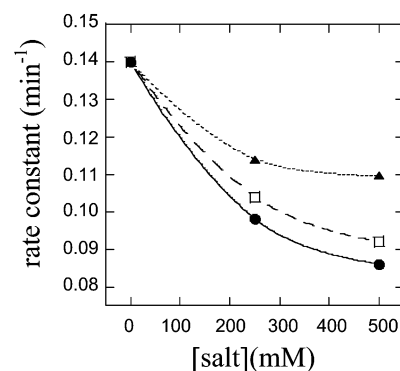


FIGURE 8: Rates of chymotrypsin digestion as a function of salt concentration and type. Plotted are the pseudo-first-order rate constants for the initial chymotrypsin cleavage event in the  $\alpha$  subunit in 50 mM MOPS, pH 7.00, 1 mM DTT, and the indicated concentration of sodium sulfate ( $\bullet$ ), sodium phosphate ( $\square$ ), and sodium chloride ( $\blacktriangle$ ). Each point represents the rate constant determined from the best fit of a time course of chymotrypsin proteolysis to eq 3.

as the observed stabilization of the  $\alpha$  subunit second unfolding transition (Figure 7B).

**Effect of Salts on the Native State of the  $\alpha$  Subunit.** The rate of digestion of the  $\alpha$  subunit by chymotrypsin decreased as the salt concentration was increased. Figure 8 shows the observed pseudo-first-order rate constant for the first chymotrypsin cleavage event of the  $\alpha$  subunit as a function of increasing concentrations of  $Na_2SO_4$ , sodium phosphate, and NaCl. The order of effectiveness of the sodium salts in decreasing the rate of proteolysis followed the same order

as was observed for the stabilization observed in the equilibrium denaturation experiments (Figures 4 and 5).

It has previously been shown that the  $\alpha$  subunit forms a weakly associating homodimer under solution conditions similar to those employed here (12). The effect of salt on the structure and stability of the  $\alpha$  subunit could be due, at least in part, to the dimerization equilibrium, if there were an effect of salt on the equilibrium. However, sedimentation equilibrium experiments in high and low salt concentration revealed that the monomer–dimer equilibrium was unaffected by salt concentration or type (data not shown).

## DISCUSSION

Bacterial luciferase is an unusual flavin monooxygenase because it uses flavin as a substrate rather than a tightly bound cofactor. The active site of bacterial luciferase is believed to reside primarily, if not exclusively, on the  $\alpha$  subunit (see ref 25 for a review). The anion binding site, identified in the  $\alpha$  subunit in the 2.4 Å luciferase crystal structure, is in close proximity to the proposed active site (2). Even though no bacterial luciferase crystal structures have been solved with bound substrates, the location of the flavin binding site is well supported by both modeling and mutational studies (2, 26–29). Arginine 107 of the  $\alpha$  subunit appears to be the only side chain ligand bound to the anion (2). Site directed mutations of  $\alpha$ R107 to an alanine, serine, or glutamate all show increases in  $K_m$  for FMNH<sub>2</sub> (27, 30). In a recent study, Lin et al. have clearly shown that the  $\alpha$  R107E mutation eliminates the ability of phosphate ion to stimulate light emission when reduced riboflavin is used as the flavin substrate (27). However, the conservative  $\alpha$  R107K mutation shows a larger stimulation than does wild type (27). Phosphate ion has been shown to compete with the binding of FMNH<sub>2</sub> (14).

Observation of an anion bound to the  $\alpha$  subunit in the 2.4 Å luciferase crystal structure suggested a method for testing the proposed two domain folding model in the context of the entire polypeptide (12). The binding site of the anion is located within the proposed N-terminal folding domain (2, 12). On the basis of the model, the expected effect of increasing the anion concentration would be to shift the second unfolding transition to higher denaturant concentration due to binding-induced stabilization (Figure 2B). The results agreed with the prediction for each anion tested (phosphate, sulfate, and chloride). Therefore, the effect of salts on the folding of the  $\alpha$  subunit was consistent with the two-domain folding hypothesis, with the second transition representing the unfolding of the N-terminal domain. The stabilization did not appear to arise from the increase in ionic strength, as correcting for the valency of the salts did not change the order of the stabilizing effect. Varying the cation of the sulfate salts tested had minimal effect on stabilization, implying that the anions were responsible for the observed stabilization of the  $\alpha$  subunit. Multivalent anions had the largest stabilizing effect, as would be predicted on the basis of the observed anion binding site in the crystal structure (2).

Removal of the C-terminal folding domain of the  $\alpha$  subunit by limited chymotrypsin treatment followed by anion exchange chromatography resulted in an N-terminal fragment of  $\alpha$ , the  $\gamma$  fragment, that refolded cooperatively upon dilution out of urea (Figure 7). The  $\gamma$  fragment refolded by an apparent two-state mechanism with a midpoint approximating

that of the  $\alpha$  subunit second unfolding transition as would be predicted from the model proposed by Noland et al. (12). Apparent two-state refolding behavior of N-terminally derived fragments has been observed in other TIM barrel proteins with similar proposed folding mechanisms (31, 32). Because the  $\gamma$  fragment contains the anion binding site (Figure 3), it would be expected to show stabilization in the presence of anions in a manner similar to the second unfolding transition for the  $\alpha$  subunit. As predicted from the proposed model, the presence of 400 mM phosphate during refolding of the  $\gamma$  fragment caused roughly the same shift in the transition midpoint as was observed for the second unfolding transition of the  $\alpha$  subunit (Figure 7B). The folding studies on the isolated N-terminal domain thus are consistent with the proposed model (Figures 1 and 2).

Multivalent anions have been shown to reduce the protease lability of luciferase as well as protect the enzyme from thermal and urea-induced denaturation (15, 16). The results of limited proteolysis of the free  $\alpha$  subunit by chymotrypsin in the presence of various salts presented in this study were consistent with previously published proteolysis results for  $\alpha\beta$  (15, 16). The order of effectiveness of the anions for  $\alpha$  subunit stabilization followed the same order of stabilization found for luciferase stabilization (15). It is interesting that, in the 2.4 Å crystal structure, residues 272–288 are not observed in the  $\alpha$  subunit electron density map (Figure 3, dashed line) (2). This region of the  $\alpha$  subunit has been shown to be labile to a number of different protease activities (see ref 25 for a review). On the other hand, in the 1.5 Å resolution luciferase crystal structure, residues 262–292 of the  $\alpha$  subunit are disordered (3). The crystals used to determine this structure were grown under low salt conditions in the absence of phosphate or sulfate salts, and no electron density was observed in the anion binding site. The results suggest that binding of the anion observed in the lower resolution luciferase crystal structure (2) may order an additional 14 residues of the  $\alpha$  subunit protease labile region compared with the higher resolution crystal structure solved using crystals grown under low salt conditions (3). Alternatively, the observed difference in the extent of the disordered loop in the two crystals could be the result of differences in crystal packing. Nonetheless, anion-induced ordering of the protease labile loop of the  $\alpha$  subunit is likely the reason that the rates of chymotrypsin proteolysis decrease with increasing salt concentration in both luciferase and the free  $\alpha$  subunit. Flavin binding has also been shown to decrease the rate of proteolytic inactivation of bacterial luciferase (15, 33).

Meighen and MacKenzie have demonstrated that salt binding enhances the bioluminescence quantum yield when neutral flavin analogues of FMN are used as substrates in luciferase assays (14). Ion binding has little effect on the binding constants for these uncharged flavin analogues but dramatically improves the efficiency of the bioluminescence reaction with these substrates. The bioluminescence reaction is optimal when a negative charge is placed approximately 8.4 Å away from the N-10 position of the flavin ring (14). With the neutral flavin analogues as substrates, Meighen and MacKenzie showed that sulfate had the largest stimulatory effect on light emission, followed by phosphate, while chloride had very little effect (14). This was the same order of effectiveness of the anions observed here for  $\alpha$  subunit stabilization through anion binding. The binding of anions was shown to be competitive with the binding of the



phosphate moiety of the flavin substrate (14), consistent with binding at the same site, in good agreement with mutagenesis studies at  $\alpha$ R107 (27, 30).

Salts are thought to stabilize proteins by several different mechanisms including specific and nonspecific binding and through changing water structure (34). The Hofmeister series is a ranking of various salts on the basis of the ability of the ions to decrease the solubility of proteins while stabilizing the native state (35). Hofmeister ion interactions are thought to occur by the weak interaction model and not through specific ion binding (36). For proteins observed to be stabilized by salts, binding versus Hofmeister stabilization is typically determined by the rank ordering of the salts with respect to stabilization (37–39). Binding is assumed when the rank order of most to least stabilizing salt follows the electroselectivity series for binding to ion-exchange resins and not the Hofmeister series (35). The  $\alpha$  subunit of bacterial luciferase represents a case where using the rank ordering of most to least stabilizing ions could lead to an incorrect interpretation regarding the mechanism of salt stabilization. The order of anions from most to least stabilizing was found to be  $\text{SO}_4 > \text{PO}_4 \gg \text{Cl}$ , which follows the Hofmeister series; however, on the basis of the observation of a phosphate or sulfate ion bound to the  $\alpha$  subunit in the 2.4 Å luciferase crystal structure, phosphate and/or sulfate would be expected to bind this site better than chloride.

There are many examples in the literature of proteins that require a ligand to fold into the proper native conformation. The folding of ribonuclease P (40) and of zinc finger domains (41, 42) requires ligand binding for proper folding. There are also many examples of proteins which do not require ligands to fold but are stabilized by ligand binding. RNase T1 (43), Sac 7d (38), and  $\alpha$ -lactalbumin (44) and dihydrofolate reductase (45) are examples. Anion binding to human serum albumin preferentially stabilizes the first unfolding transition but not the second (39). Bovine serum albumin (BSA) is a multidomain protein that unfolds in a multistep process when titrated with urea. Domain specific ligands to BSA were used by Tayyab et al. to probe the stability of the individual domains in the context of the intact protein (46). The two domains of calmodulin have different affinities for calcium and magnesium and so the N- and C-terminal domain stabilities can be preferentially tuned by the addition of either calcium or magnesium (47). Pigeon liver malic enzyme shows domain-specific stabilization in the presence of  $\text{Mn}^{2+}$  ions (48). The NK1 fragment of plasminogen contains a domain that is preferentially stabilized in the presence of *trans*-(aminomethyl)cyclohexanecarboxylic acid (49).

There are several examples in the literature of TIM barrels that show non-two-state unfolding and refolding behavior besides bacterial luciferase. The TIM barrel enzymes involved in tryptophan biosynthesis, the  $\alpha$  subunit of tryptophan synthase ( $\alpha$ -TS), indoleglycerol phosphate synthase (IGPS), and phosphoribosyl anthranilate isomerase (PRAI) all have been shown to have at least one equilibrium folding intermediate (32, 50–52). The folding of  $\alpha$ -TS has been shown to occur through two equilibrium intermediates (52). Fragmentation studies of  $\alpha$ -TS and PRAI have identified probable N- and C-terminal folding domains consisting of the first six  $\beta$  strands and the last two respectively (31, 32). For these two proteins the first transition represents the unfolding of the C-terminal domain and the second transition

represents the unfolding of the N-terminal domain. A similar fragmentation approach has not been conducted on IGPS, but equilibrium folding studies suggest that a similar folding mechanism may give rise to the observed three-state unfolding (51).  $\alpha$ -TS, PRAI, and IGPS all bind phosphate-containing substrates, and the phosphate binding sites lie in the proposed C-terminal folding domains. Therefore, increasing the anion concentration would be expected to stabilize the C-terminal folding domains of these TIM barrel proteins. For  $\alpha$ -TS, PRAI, and possibly IGPS the predicted effect of increasing phosphate or sulfate ion concentration would be a shift of the first unfolding transition to higher urea concentrations as diagrammed in Figure 2A.

On the basis of the studies reported here and the results of others, discussed above, it would appear that the proposal of Wetlaufer (1) to dissect the study of folding of large multidomain proteins into smaller, more manageable, efforts to understand the folding and stability of the domains was well founded. At least in the cases described here, individual folding domains are stabilized specifically by binding of ligands to the specific domain.

## ACKNOWLEDGMENT

The authors acknowledge Drs. Jonathan Sparks, Jennifer Inlow, Michael Thomas, and Anita van Tilburg for helpful discussions, advice, and encouragement. We also thank Dr. Miriam Ziegler for critical reading of this manuscript.

## REFERENCES

1. Wetlaufer, D. B. (1981) Folding of protein fragments. *Adv. Protein Chem.* 34, 61–92.
2. Fisher, A. J., Raushel, F. M., Baldwin, T. O., and Rayment, I. (1995) Three-dimensional structure of bacterial luciferase from *Vibrio harveyi* at 2.4 Å resolution. *Biochemistry* 34, 6581–6586.
3. Fisher, A. J., Thompson, T. B., Thoden, J. B., Baldwin, T. O., and Rayment, I. (1996) The 1.5-Å resolution crystal structure of bacterial luciferase in low salt conditions. *J. Biol. Chem.* 271, 21956–21968.
4. Ziegler, M. M., Goldberg, M. E., Chaffotte, A. F., and Baldwin, T. O. (1993) Refolding of luciferase subunits from urea and assembly of the active heterodimer. Evidence for folding intermediates that precede and follow the dimerization step on the pathway to the active form of the enzyme. *J. Biol. Chem.* 268, 10760–10765.
5. Baldwin, T. O., Ziegler, M. M., Chaffotte, A. F., and Goldberg, M. E. (1993) Contribution of folding steps involving the individual subunits of bacterial luciferase to the assembly of the active heterodimeric enzyme. *J. Biol. Chem.* 268, 10766–10772.
6. Clark, A. C., Raso, S. W., Sinclair, J. F., Ziegler, M. M., Chaffotte, A. F., and Baldwin, T. O. (1997) Kinetic mechanism of luciferase subunit folding and assembly. *Biochemistry* 36, 1891–1899.
7. Clark, A. C., Sinclair, J. F., and Baldwin, T. O. (1993) Folding of bacterial luciferase involves a non-native heterodimeric intermediate in equilibrium with the native enzyme and the unfolded subunits. *J. Biol. Chem.* 268, 10773–10779.
8. Sinclair, J. F., Ziegler, M. M., and Baldwin, T. O. (1994) Kinetic partitioning during protein folding yields multiple native states. *Nat. Struct. Biol.* 1, 320–326.
9. Sinclair, J. F., Waddle, J. J., Waddill, E. F., and Baldwin, T. O. (1993) Purified native subunits of bacterial luciferase are active in the bioluminescence reaction but fail to assemble into the alpha beta structure. *Biochemistry* 32, 5036–5044.
10. Thoden, J. B., Holden, H. M., Fisher, A. J., Sinclair, J. F., Wesenberg, G., Baldwin, T. O., and Rayment, I. (1997) Structure of the  $\beta_2$  homodimer of bacterial luciferase from *Vibrio harveyi*: X-ray analysis of a kinetic protein folding trap. *Protein Sci.* 6, 13–23.
11. Tanner, J. J., Miller, M. D., Wilson, K. S., Tu S.-C., and Krause, K. L. (1997) Structure of bacterial luciferase  $\beta_2$  homodimer: implications for flavin binding. *Biochemistry* 36, 665–672.

12. Noland, B. W., Dangott, L. J., and Baldwin, T. O. (1999) Folding, stability, and physical properties of the alpha subunit of bacterial luciferase. *Biochemistry* 38, 16136–16145.
13. Noland, B. W. (2001) Characterization of the thermodynamic and kinetic folding mechanism of the  $\alpha$  subunit of bacterial luciferase. Ph.D. Thesis, Texas A&M University, College Station, TX.
14. Meighen, E. A., and MacKenzie, R. E. (1973) Flavine specificity of enzyme–substrate intermediates in the bacterial bioluminescent reaction. Structural requirements of the flavine side chain. *Biochemistry* 12, 1482–1491.
15. Baldwin, T. O., and Riley, P. L. (1980) Anion binding to bacterial luciferase: evidence for binding associated changes in enzyme structure, in *Flavins and Flavoproteins* (Yagi, K., and Yamano, T., Eds.) pp 139–147, University Park Press, Baltimore, MD.
16. Holzman, T. F., and Baldwin, T. O. (1980) Proteolytic inactivation of luciferases from three species of luminous marine bacteria, *Beneckeia harveyi*, *Photobacterium fischeri*, and *Photobacterium phosphoreum*: evidence of a conserved structural feature. *Proc. Natl. Acad. Sci. U.S.A.* 77, 6363–6367.
17. Cohn, D. H., Mileham, A. J., Simon, M. I., Neelson, K. H., Rausch, S. K., Bonam, D., and Baldwin, T. O. (1985) Nucleotide sequence of the *luxA* gene of *Vibrio harveyi* and the complete amino acid sequence of the  $\alpha$  subunit of bacterial luciferase. *J. Biol. Chem.* 260, 6139–6146.
18. Rausch, S. K., Dougherty, J. I., Jr., and Baldwin, T. O. (1982) Structural analysis of fragments resulting from limited proteolysis of bacterial luciferase, in *Flavins and Flavoproteins* (Massey, V., and Williams, C. H., Eds.) pp 375–378, Elsevier North-Holland, Inc., New York.
19. Baldwin, T. O., Ziegler, M. M., Green, V. A., and Thomas, M. D. (2000) Overexpression of bacterial luciferase and purification from recombinant sources. *Methods Enzymol.* 305, 135–152.
20. Thomas, M. D., and van Tilburg, A. (2000) Overexpression of foreign proteins using the *Vibrio fischeri lux* control system. *Methods Enzymol.* 305, 315–329.
21. Royer, C. A., Mann, C. J., and Matthews, C. R. (1993) Resolution of the fluorescence equilibrium unfolding profile of trp aporepressor using single tryptophan mutants. *Protein Sci.* 2, 1844–1852.
22. Santoro, M. M., and Bolen, D. W. (1988) Unfolding free energy changes determined by the linear extrapolation method. Unfolding of phenylmethanesulfonyl alpha-chymotrypsin using different denaturants. *Biochemistry* 27, 8063–8068.
23. Cohn, E. J., and Edsall, J. T. (1943) *Proteins, amino acids, and peptides as ions and dipolar ions*, pp 370–381, Reinhold, New York.
24. Laue, T. P., Bhairavi, D. S., Ridgeway, T. M., and Pelletier, S. L. (1992) in *Analytical Ultracentrifugation in Biochemistry and Polymer Science* (Harding, S. E., Rowe, A. J. H., and Horton, J. C., Eds.) pp 63–89, The Royal Society of Chemistry, Cambridge, U.K.
25. Baldwin, T. O., and Ziegler, M. M. (1992) The biochemistry and molecular biology of bacterial bioluminescence, in *Chemistry and Biochemistry of Flavoproteins* (Müller, F., Ed.) pp 467–530, CRC Press, Boca Raton, FL.
26. Raso, S. W. (1997) The use of mutant enzymes to probe the structure, function and folding pathway of bacterial luciferase. Ph.D. Thesis, Texas A&M University, College Station, TX.
27. Lin, L. Y.-C., Sulea, T., Szittner, R., Vassilyev, V., Purisima, E. O., and Meighen, E. A. (2001) Modeling of the bacterial luciferase-flavin mononucleotide complex combining flexible docking with structure–activity data. *Protein Sci.* 10, 1563–1571.
28. Clark, A. C. (1994) Thermodynamic and kinetic studies of the polypeptide folding of bacterial luciferase from *Vibrio harveyi*: a mutational analysis. Ph.D. Thesis, Texas A&M University, College Station, TX.
29. Li, Z., and Meighen, E. A. (1995) Tryptophan 250 on the alpha subunit plays an important role in flavin and aldehyde binding to bacterial luciferase. Effects of W  $\rightarrow$  Y mutations on catalytic function. *Biochemistry* 34, 15084–15090.
30. Moore, C., Lei, B., and Tu, S.-C. (1999) Relationship between the conserved alpha subunit arginine 107 and effects of phosphate on the activity and stability of *Vibrio harveyi* luciferase. *Arch. Biochem. Biophys.* 370, 45–50.
31. Miles, E. W., Yutani, K., and Ogasahara, K. (1982) Guanidine hydrochloride induced unfolding of the  $\alpha$  subunit of tryptophan synthase and two proteolytic fragments: Evidence for stepwise unfolding of the two domains. *Biochemistry* 21, 2586–2592.
32. Elder, J., and Kirschner, K. (1992) Stable substructures of 8-fold  $\alpha\beta$ -barrel proteins: Fragment complementation of phosphoribosylanthranilate isomerase. *Biochemistry* 31, 3617–3625.
33. AbouKhair, N. K., Ziegler, M. M., and Baldwin, T. O. (1985) Bacterial luciferase: demonstration of a catalytically competent altered conformational state following single turnover. *Biochemistry* 24, 3942–3947.
34. Jencks, W. P. (1969) Electrostatic Interactions, in *Catalysis in Chemistry and Enzymology*, pp 351–375, McGraw-Hill Book Co., New York.
35. Collins, K. D., and Washabaugh, M. W. (1985) The Hofmeister effect and the behaviour of water at interfaces. *Quantum Rev. Biophys.* 4, 323–422.
36. Baldwin, R. L. (1996) How Hofmeister ion interactions affect protein stability. *Biophys. J.* 71, 2056–2063.
37. Goto, Y., Takahashi, N., and Fink, A. (1990) Mechanism of acid-induced folding of proteins. *Biochemistry* 29, 3480–3488.
38. McCrary, B. S., Bedell, J., Edmondson, S. P., and Shriver, J. W. (1998) Linkage of protonation and anion binding to the folding of Sac7d. *J. Mol. Biol.* 276, 203–224.
39. Muzammil, S., Kumar, Y., and Tayyab, S. (2000) Anion-induced stabilization of human serum albumin prevents the formation of intermediate during urea denaturation. *Proteins: Struct., Funct., Genet.* 40, 29–38.
40. Henkels, C. H., Kurz, J. C., Fierke, C. A., and Oas, T. G. (2001) Linked folding and anion binding of the *Bacillus subtilis* ribonuclease P protein. *Biochemistry* 40, 2777–2789.
41. Frankel, A. D., Berg, J., and Pabo, C. O. (1987) Metal-dependent folding of a single zinc finger from transcription factor IIIA. *Proc. Natl. Acad. Sci. U.S.A.* 84, 4841–4845.
42. Parraga, G., Horath, S. J., Eisen, A., Taylor, W. E., Hood, L., Young, E. T., and Klevit, R. E. (1988) Zinc-dependent structure of a single-finger domain of yeast ADR1. *Science* 241, 1489–1492.
43. Pace, C. N., and Grimsley, G. R. (1988) Ribonuclease T1 is stabilized by cation and anion binding. *Biochemistry* 27, 3242–3246.
44. Hiraoka, Y., Segawa, T., Kawajima, K., Sugai, S., and Murai, N. (1980)  $\alpha$ -Lactalbumin: a calcium metalloprotein. *Biochem. Biophys. Res. Commun.* 95, 1098–1104.
45. Hillcoat, B. L., Marshall, L., Gauldie, J., and Hiebert, M. (1971) Stabilization of dihydrofolate reductase by inhibitors in vivo and in vitro. *Ann. N.Y. Acad. Sci.* 186, 187–208.
46. Tayyab, S., Sharma, N., and Khan, M. M. (2000) Use of domain specific ligands to study urea-induced unfolding of bovine serum albumin. *Biochem. Biophys. Res. Commun.* 227, 83–88.
47. Masino, L., Martin, S. R., and Bayley, P. M. (2000) Ligand binding and thermodynamic stability of a multidomain protein, calmodulin. *Protein Sci.* 9, 1519–1529.
48. Chang, H. C., Chou, W. Y., and Chang, G. G. (2002) Effect of metal binding on the structural stability of pigeon liver malic enzyme. *J. Biol. Chem.* 277, 4663–4671.
49. Douglas, J. T., von Haller, P. D., Gehrman, M., Llinas, M., and Schaller, J. (2002) The two-domain NK1 fragment of plasminogen: folding, ligand binding, and thermal stability profile. *Biochemistry* 41, 3302–3310.
50. Matthews, C. R., and Crisanti, M. M. (1981) Urea-induced unfolding of the alpha subunit of tryptophan synthase: evidence for a multistate process. *Biochemistry* 20, 784–792.
51. Sánchez del Pino, M. M., and Fersht, A. R. (1997) Nonsequential unfolding of the  $\alpha\beta$  barrel protein indole-3-glycerol-phosphate synthase. *Biochemistry* 36, 5560–5565.
52. Gualfetti, P. J., Bisel, O., and Matthews, C. R. (1999) The progressive development of structure and stability during equilibrium folding of the  $\alpha$  subunit of tryptophan synthase from *Escherichia coli*. *Protein Sci.* 8, 1623–1635.
53. Christopher, J. A. (1998) *SPOCK: The Structural Properties Observation and Calculation Kit* (Program Manual) pp 1–131, The Center for Macromolecular Design, Texas A&M University, College Station, TX.
54. Kraulis, P. J. (1991) MOLSCRIPT: a program to produce both detailed and schematic plots of protein structures. *J. Appl. Crystallogr.* 24, 946–950.